

STAT3 inhibition prevents lung inflammation, remodeling, and accumulation of Th2 and Th17 cells in a murine asthma model

A. C. Gavino¹, K. Nahmod², U. Bharadwaj³, G. Makedonas² & D. J. Tweardy^{3,4,5}

¹Section of Immunology, Allergy and Rheumatology, Department of Medicine, Baylor College of Medicine; ²Center for Human Immunobiology, Department of Pediatrics, Texas Children's Hospital, Baylor College of Medicine; ³Section of Infectious Disease, Department of Medicine, Baylor College of Medicine; ⁴Department of Cellular and Molecular Biology, Baylor College of Medicine; ⁵Department of Biochemistry and Molecular Biology, Baylor College of Medicine, Houston, TX, USA

To cite this article: Gavino AC, Nahmod K, Bharadwaj U, Makedonas G, Tweardy DJ. STAT3 inhibition prevents lung inflammation, remodeling, and accumulation of Th2 and Th17 cells in a murine asthma model. *Allergy* 2016; DOI: 10.1111/all.12937.

Keywords

airway inflammation; asthma; cytokines; lymphocytes; STAT3.

Correspondence

Dr. David J. Tweardy, M.D., University of Texas MD Anderson Cancer Center, 1400 Pressler Street, FCT12.5069, Unit 1463, Houston, TX 77030-3772, USA.
Tel.: +1 713 792-6517
Fax: +1 713 792-3029
E-mail: djtweardy@mdanderson.org

Accepted for publication 21 May 2016

DOI:10.1111/all.12937

Edited by: Angela Haczku

Abstract

Background: STAT3 drives development of Th17 cells and cytokine production by Th2 and Th17 cells, which contribute to asthma. Alternative asthma treatments are needed, especially for the Th17 phenotype. We sought to determine whether C188-9, a small-molecule STAT3 inhibitor, can block Th2 and Th17 cell expansion and cytokine production to prevent house dust mite (HDM)-induced airway inflammation and remodeling.

Methods: Three groups of C57BL/6 mice were treated intranasally (IN) and intraperitoneally (IP) daily for 3 weeks with the following: (i) vehicle 1 IN and vehicle 2 IP, (ii) HDM IN and vehicle 2 IP, or (iii) HDM IN and C188-9 IP. Sections of lung were stained with Alcian Blue/PAS and examined microscopically. Total (t) STAT3, STAT3 phosphorylated on Y705 (pSTAT3), IL-17, IL-13, IL-5, and IL-4 levels were measured in lung protein extracts and serum using Luminex beads. Frequencies of Th2-type and Th17-type lymphocytes were assessed in lungs and bronchoalveolar lavage fluid (BALF) by multiparametric flow cytometry.

Results: HDM inhalation markedly increased airway goblet cell numbers and thickness of the epithelium and subepithelial smooth muscle layer, which was accompanied in the whole lung by increased pSTAT3, IL-4, IL-5, IL-13, and IL-17, and % CD4⁺ T cells that produce IL-5, IL-13, and IL-17. HDM inhalation also increased serum IL-4 and IL-17 levels and increased BALF % CD4⁺ T cells that produce IL-5 and IL-13. Remarkably, treatment with C188-9 normalized each endpoint.

Conclusion: HDM-induced airway inflammation, remodeling, and Th2/Th17-type cell accumulation involve STAT3 activation that can be prevented by C188-9 treatment.

Asthma affects 10% of the population worldwide and its prevalence has been increasing over the last decade (1).

Abbreviations

BAL, bronchoalveolar lavage; DMSO, dimethyl sulfoxide; GAPDH, glyceraldehyde-3-phosphate dehydrogenase; HDM, house dust mite; HNSCC, head and neck squamous cell carcinoma; IN, intranasal; IP, intraperitoneal; PBS, phosphate buffer saline; pSTAT, phosphotyrosylated signal transducer and activator of transcription; STAT, signal transducer and activator of transcription; tSTAT, total signal transducer and activator of transcription.

Asthma is a heterogeneous disease with multiple variants, the most widely recognized of which is the Th2 phenotype, characterized by atopy, eosinophilia, and responsiveness to steroids (2–4). However, as many as 10% of patients have the Th17 phenotype of asthma which is nonatopic, neutrophilic, and steroid resistant (5–7) resulting in a higher morbidity and mortality owing to the lack of available effective treatments (6, 8). Alternative therapeutic options clearly are needed for this subset of patients.

Signal transducer and activator of transcription 3 (STAT3) is essential for Th17 lymphocyte development and cytokine

production, and its activation is linked to the development of airway inflammation (9, 10). Upon activation, STAT3 is recruited to cytokine-activated receptor complexes and becomes phosphorylated at Tyr (Y) 705. Phosphotyrosylated (p) STAT3 homodimerizes through reciprocal SH2-pY705 interactions, translocates to the nucleus, and binds to promoters to transcriptionally activate genes that drive Th17 differentiation and production of multiple cytokines (11, 12). STAT3 activation also is involved in Th2 cytokine production (13–16), making it an attractive target for asthma treatment.

C188-9 is a small-molecule probe designed to target the SH2 domain of STAT3 and prevent activation of STAT3 by blocking its recruitment to cytokine-activated receptor complexes, Y705 phosphorylation, and homodimerization (17–19). Here we demonstrate that STAT3 inhibition with C188-9 can prevent the development of airway inflammation by blocking Th2 and Th17 lymphocyte accumulation and cytokine production in the lung of mice subjected to the murine model of house dust mite (HDM)-induced asthma.

Methods

Animals

Male C57BL/6 mice were purchased from Harlan Laboratories (Indianapolis, IN, USA). These mice were housed in a pathogen-free environment. The Baylor College of Medicine IACUC approved all aspects of the animal protocols used in this study.

C188-9 and mouse HDM protocols

C188-9 was obtained from StemMed, Ltd. (Houston, TX, USA). In plasma and tissue pharmacokinetic studies in mice, C188-9 achieved a plasma C_{max} of 14.5 μ M and a plasma half-life of 90 min following intraperitoneal (IP) administration (10 mg/kg), which resulted in plasma levels exceeding the IC_{50} for inhibition of cytokine-mediated STAT3 activation (3 μ M) for ~3 h (20). C188-9 also was concentrated in tumor tissue to levels 2.2-fold higher than simultaneously obtained serum (20). In studies examining the pharmacodynamics of C188-9 in mice, we determined that constitutively elevated levels of pSTAT3 in tumor xenografts were reduced for at least 24 h after administration of C188-9 (50 mg/kg; Fig. S1). C188-9 previously was demonstrated not to target kinases known to activate STAT3 (17). To determine the specificity of C188-9 for STAT3 vs STAT5 and STAT6, which also has been implicated in asthma development, we examined its ability to reduce tyrosine-phosphorylated STAT protein (pSTAT) levels in two respiratory epithelial tumor cell lines—head and neck squamous cell carcinoma (HNSCC) cell lines SQ-20B and SCC-35—that demonstrated increased levels of pSTAT3, pSTAT5, and pSTAT6 (Fig. S2A). In each cell line, C188-9 decreased the levels of pSTAT3 but not the levels of pSTAT5 or pSTAT6 (Fig. S2B).

To examine the effect of C188-9 in a murine model of asthma, fifty-one mice were divided into three groups of 17

each (Fig. S3). Mice in each group received intranasal (IN) and intraperitoneal (IP) treatments for 5 days (Monday through Friday) per week for 3 weeks, as follows. The first group [HDM(–) C188(–)] received vehicle 1 (PBS/10% DMSO, 25 μ l) IN and vehicle 2 (5% dextrose in water containing 10% DMSO and 50% PEG400, 200 μ l) by IP injection. The second group [HDM(+) C188(–)] received HDM extract (1.6 mg/ml in vehicle 1, 25 μ l) and vehicle 2 (200 μ l) IP. The third group [HDM(+) C188(+)] received HDM extract IN and C188-9 (50 mg/kg in vehicle 2, 200 μ l) IP. IN administration consisted of drop-wise placement of vehicle 1 with or without HDM extract into alternating nostrils of an isoflurane-anesthetized mouse. Intraperitoneal (IP) injections were administered to the right lower quadrant of the abdomen of mice using a 27-gauge needle.

On the final treatment day, each mouse was killed 1 h after administration of the last dose of HDM, C188-9, and/or vehicle. In 10 mice per group, blood was harvested by cardiac puncture using a 27-gauge needle. Blood was allowed to clot for 30 min and then centrifuged for 10 min at 1000 \times g. Serum was harvested immediately and frozen in aliquots. Lungs were harvested and split into left and right lungs. Left lungs were inflated, fixed in 4% paraformaldehyde for 24 h, and then paraffin embedded. Right lungs were snap-frozen in liquid nitrogen.

In another set of experiments with seven mice/group, bronchoalveolar lavage (BAL) was performed, as previously described (15). After cardiac puncture for terminal collection of a large blood volume, lungs were harvested sparing the peritracheal lymph nodes. Lungs were washed twice with RPMI 1640 (GIBCO; Life Technologies, Carlsbad, CA, USA), mechanically disrupted, and filtered through a 70- μ m cell strainer (BD Falcon; BD Biosciences, Bedford, MA, USA) to remove major tissue fragments. To isolate the mononuclear cells, lung single-cell suspensions were layered onto Ficoll-Paque Premium 1.084 (GE Healthcare, Pittsburgh, PA, USA) and centrifuged following the manufacturer's instructions. Cells at the interface were washed twice with Dulbecco's PBS, counted, and assessed for viability using an automated cell counter (Nexcelom Bioscience, Lawrence, MA, USA).

Histological analysis of airway inflammation

Five-micron sections of lungs in paraffin blocks were placed on slides, stained with Alcian Blue–Periodic Acid-Schiff (PAS) (Waltham, MA, USA), and examined microscopically under 400 \times magnification using an Olympus BX46 microscope (Center Valley, PA, USA). Round airways of equivalent size were randomly selected within each lung section. Images were captured using an Olympus DP26 camera (Center Valley, PA, USA). Olympus cellSens standard software (version 1.6) was used to take measurements of the digitalized images. The number of goblet cells in each airway was counted and divided by the circumference of the basement membrane, and the number was multiplied by 100. The thickness of the epithelial layer and the subepithelial smooth muscle layer was measured in each airway at four different

points and the mean thickness was calculated. The investigator performing the microscopy and image analysis was blinded to the treatment the mouse received.

Lung and serum analyte measurements

Flash-frozen lung was homogenized, centrifuged, and supernatants collected as lysates. Protein concentrations within lysates were determined by Bradford assay. Luminex bead-based assays were performed in duplicate on lung lysates (standardized to 1 mg protein/ml) and on serum to determine the levels of IL-17 (Th17 cytokine) and Th2 cytokines (IL-13, IL-5, and IL-4). Luminex bead assays also were performed in duplicate on lung lysates to determine the levels of pSTAT3 and total (t) STAT3. Analyte values in lung lysates were normalized to total protein concentration.

Flow cytometry

Mononuclear cells obtained from BAL fluid and whole-lung homogenates were re-suspended in complete medium (RPMI 1640, 10%FBS, L-glutamine, penicillin/streptomycin) and cultured overnight at a density of $0.5-1 \times 10^6$ cells/ml in the presence of house dust mite 5 µg/ml and brefeldin 10 µg/ml (Sigma, St. Louis, MO, USA). After 12 h, cells were washed, incubated with Ghost viability dye (Tonbo Biosciences, San Diego, CA, USA), and incubated with anti-CD3e APC-Cy7 clone 145-2c11 (Tonbo Biosciences), anti-CD4 PE-Cy5 clone RM4-5 (BD Biosciences, Bedford, MA, USA), and anti-CD8a BV785 clone 53-6.7 (Biolegend, San Diego, CA, USA), as described (21). Cells were washed, fixed, and permeabilized using BD Cytotfix/Cytoperm Fixation/Permeabilization solution following the manufacturer's instructions (BD Biosciences). A cocktail of antibodies each targeting a specific intracellular antigen was added and cells were incubated for 1 h at RT. The cocktail included anti-IL-4 PerCP-eFluor 710 clone 11B11, anti-IL-13 PE-Cy7 Ebio13A, anti-IL-17A FITC clone eBio17B7 (eBioscience, San Diego, CA, USA), anti-IFN- γ AF700 clone XMG1.2, anti-IL-5 PE clone TRFK5 (BD Biosciences), anti-TNF- α BV650 clone MP6-XT22, anti-IL-2 BV421 clone JEs6-5H4, and anti-IL-22 Alexa Fluor 647 Poly5164 (Biolegend). After staining, cells were washed and fixed with PFA1%. Cells were examined by flow cytometry using a BD LSR Fortessa (BD Biosciences) and data analyzed using FlowJo Software v10.0.7 (Tristar, Ashland, OR, USA).

Statistical analysis

Histological data, Luminex data, and lymphocyte frequencies were expressed as means \pm SEM. One-way analysis of variance (ANOVA) followed by Tukey's multiple comparison test was used to compare differences between the groups when analyzing lung histology and serum, lung, and BAL fluid analyte measurements. All lymphocyte data sets were tested for Gaussian distribution using Kolmogorov-Smirnov normality test. ANOVA followed by Fisher's LSD or Kruskal-

Wallis test followed by Dunn's multiple comparison posttest were used to compare lymphocyte differences, as appropriate. Statistical analyses were performed with GraphPad Prism 6 software program (La Jolla, CA, USA). A *P* value of <0.05 was considered statistically significant.

Results

Airway inflammation and remodeling in mice administered HDM are accompanied by STAT3 activation; administration of C188-9 normalized HDM-induced pSTAT3 levels and reversed airway inflammation and remodeling

It was previously demonstrated that the administration of HDM IN to C57BL/6 mice (40 µg, 5 times/week for 5 weeks) increased pSTAT3 levels in their lungs and that this was accompanied by airway inflammation, Th2 lymphocyte accumulation, chemokine production, and airway hyper-responsiveness (15). We administered PBS without or with HDM IN to 10 C57BL/6 mice (40 µg, 5 times/week for 3 weeks) to confirm and extend these findings and determined that the levels of pSTAT3 in lungs from HDM-treated mice (Fig. 1) were increased sevenfold compared to PBS-treated mice ($P < 0.05$); this increase in lung pSTAT3 was accompanied by marked airway inflammation and remodeling (Fig. 2), including a 35-fold increase in goblet cells, a sixfold increase in epithelial cell thickness, and a threefold increase in subepithelial smooth muscle thickness ($P < 0.0001$ for each). Earlier studies demonstrated that intranasal administration of two compounds (tyrphostin A1 and SU6656) capable of inhibiting kinases previously shown to activate STAT3, either alone or in combination, appeared to diminish HDM-induced increases in pSTAT3 and to reduce eosinophilic lung infiltration (15). To determine the effect of C188-9, a compound that specifically targets STAT3 in respiratory epithelial cells, on HDM-mediated increase in lung pSTAT3 and remodeling, we co-administered C188-9 IP (50 mg/Kg/d) to mice receiving HDM IN. C188-9 treatment normalized levels of pSTAT3 in lung lysates of HDM-treated mice (Fig. 1), which was accompanied by prevention of HDM-induced increases in goblet cell hyperplasia, epithelial thickness, and smooth muscle thickness (Fig. 2).

HDM-induced inflammation and remodeling are accompanied by increased levels of Th2- and Th17-type cytokines, which are normalized by C188-9 treatment

Both Th2- and Th17-type cytokines have been shown to contribute to HDM-induced airway inflammation and remodeling in BALB/c mice (22) and in A/J mice (23). To determine whether Th2-type cytokines (IL-4, IL-5, and IL-13) and Th17 type cytokines (IL-17) are increased in HDM-induced airway inflammation and remodeling in C57BL/6 mice and to determine the effect of C188-9 treatment, we measured cytokine levels in protein extracts of whole lung (Fig. 3) and serum (Fig. 4). HDM increased the levels of IL-17 by 2.7-fold ($P < 0.05$), IL-13 by 5.9-fold

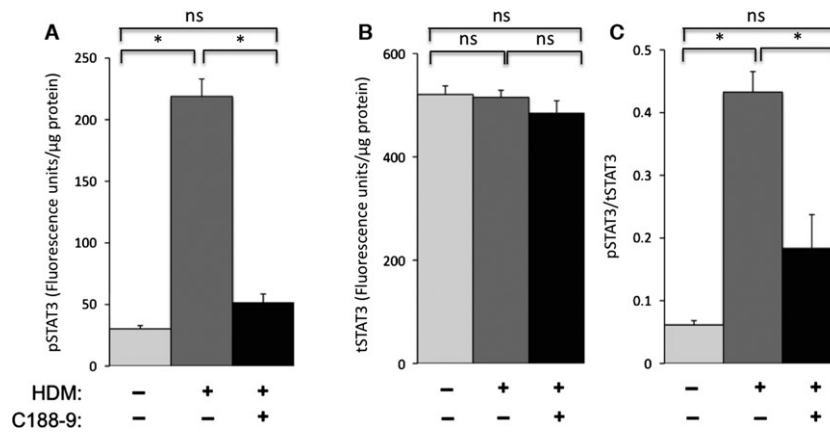


Figure 1 Effect of house dust mite and C188-9 on lung pSTAT3 (A), tSTAT3 (B), and pSTAT3/tSTAT3 (C). Proteins levels were measured using Luminex beads in lung protein extracts of mice treated as indicated. Data presented are mean ± SEM (*n* = 10. **P* < 0.05; ns, not significant).

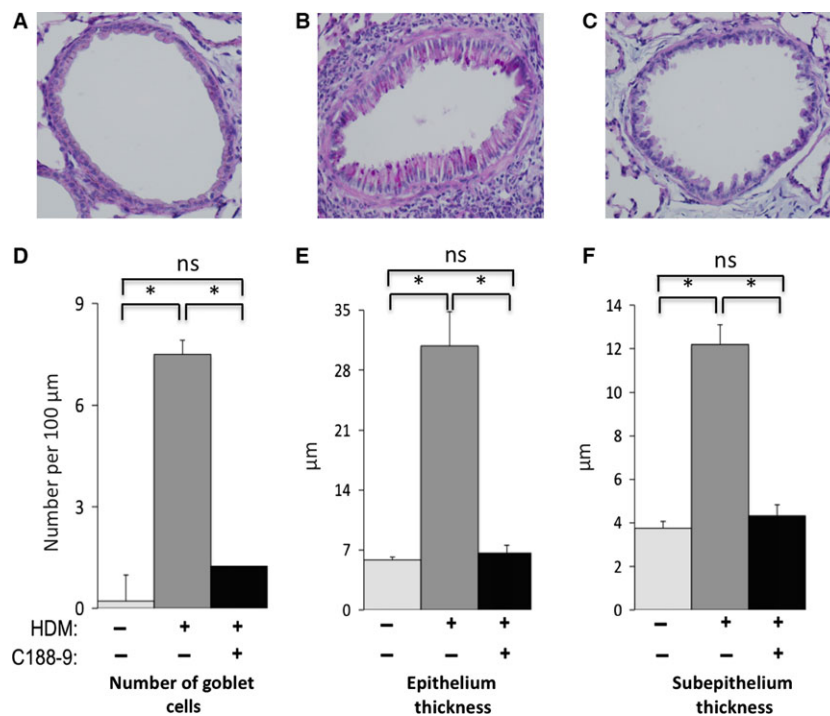


Figure 2 Effect of house dust mite (HDM) and C188-9 treatment on airway goblet cell number, epithelium thickness, and subepithelium smooth muscle thickness. Representative photomicrographs lung sections from control (A), HDM alone (B), and HDM + C188-9 mice (C) were stained with Alcian Blue-PAS and examined at 400×. Number of airway goblet cell number (D), epithelium thickness (E), and subepithelium smooth muscle thickness (F) were determined. Data presented are mean ± SEM of 10 airways per group. **P* < 0.0001; ns, not significant.

(*P* < 0.05), IL-5 by 5.8-fold (*P* < 0.05), and IL-4 by 57-fold (*P* < 0.5) in protein extracts of whole lung. Increases in lung IL-17 and IL-4 were accompanied by increases in serum IL-17 of 4.4-fold (*P* < 0.05), and in serum IL-4 of 4.6-fold (0.05); the levels of IL-5 and IL-13 were not increased in serum. Importantly, the levels of each cytokine examined were reduced to the levels statistically indistinguishable from controls in both the lungs (Fig. 3) and the

sera (Fig. 4) of HDM-treated mice that also received C188-9.

HDM treatment increased lung Th2-type and Th17-type cells, which are normalized by C188-9 treatment

To begin to determine the cellular sources of increased HDM-induced Th-2-type and Th17-type cytokines and to

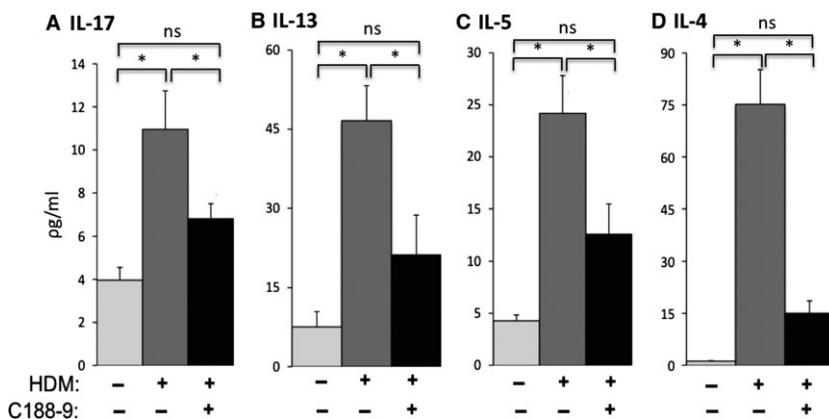


Figure 3 Effect of house dust mite and C188-9 treatment on lung levels of IL-17 (A), IL-13 (B), IL-5 (C), and IL-4 (D). Th17- and Th2-type cytokines were measured using Luminex beads in lung

protein extracts of mice treated as indicated. Data presented are mean \pm SEM. $n = 10$. * $P < 0.05$; ns, not significant.

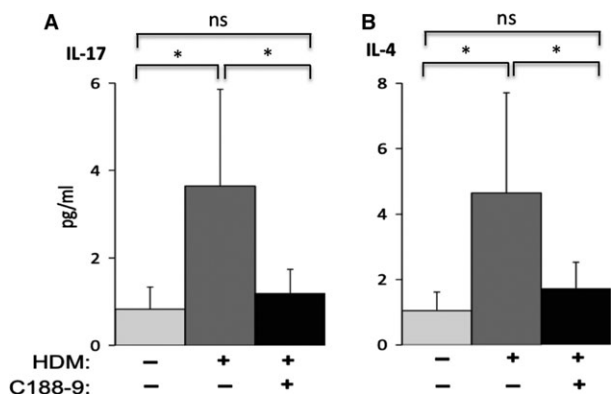


Figure 4 Effect of house dust mite and C188-9 treatment on serum IL-17 (A) and IL-4 (B). Th17 and Th2 cytokines were measured using Luminex beads in serum of mice treated as indicated. Data presented are mean \pm SEM. $n = 10$. * $P < 0.05$; ns, not significant.

within BAL fluid that produced IL-13 by 5.8-fold (from 0.17 ± 0.09 to 1.04 ± 0.4 ; $P < 0.05$; Fig. 5B) and IL-5 by 3.9-fold (from 0.25 ± 0.11 to 0.99 ± 0.23 ; $P < 0.01$; Fig. 5C); the frequency of CD4⁺ T cells in BAL fluid that produced IL-17A (Fig. 5A) or IL-4 (Fig. 5D) did not increase. Interestingly, we found that HDM induced a 3.4-fold increase in the frequency of CD3-negative cells in BAL fluid with high side scatter that produce IL-17A (from 13 ± 3.3 to 44 ± 10 ; $P < 0.05$; Fig. S4A) and a 230-fold increase in high-scatter cells that produce IL-4 (from 0.1 ± 0.06 to 23 ± 8.1 ; $P < 0.01$; Fig. S4B).

determine whether C188-9 reduced their frequency, we performed flow cytometry of both BAL fluid cells (Fig. 5) and single cell preparations of lung (Fig. 6) focusing on T cells. HDM treatment increased the frequency of CD4⁺ T cells

When CD4⁺ T cells within single-cell lung preparations were analyzed, we found that HDM increased the frequency of CD4⁺ T cells that produced IL-17A by 12-fold (from 0.19 ± 0.08 to 2.3 ± 0.88 ; $P < 0.05$; Fig. 6A), IL-13 by 5.5-fold (from 0.23 ± 0.06 to 1.28 ± 0.27 ; $P < 0.001$; Fig. 6B) and IL-5 by 7.4-fold (from 0.15 ± 0.04 to 1.12 ± 0.27 ; $P < 0.01$; Fig. 6C). Similar to the findings in BAL, we did not see an increase in the frequency of CD4⁺ T cells that produced IL-4 in the lungs (Fig. 6D). However, HDM treatment increased the frequency of CD3-negative cells with high side scatter within lung that produced IL-4 by over threefold (from 11.6 ± 3.6 to 37.8 ± 10.1 ; $P < 0.05$; Fig. 6H) and that

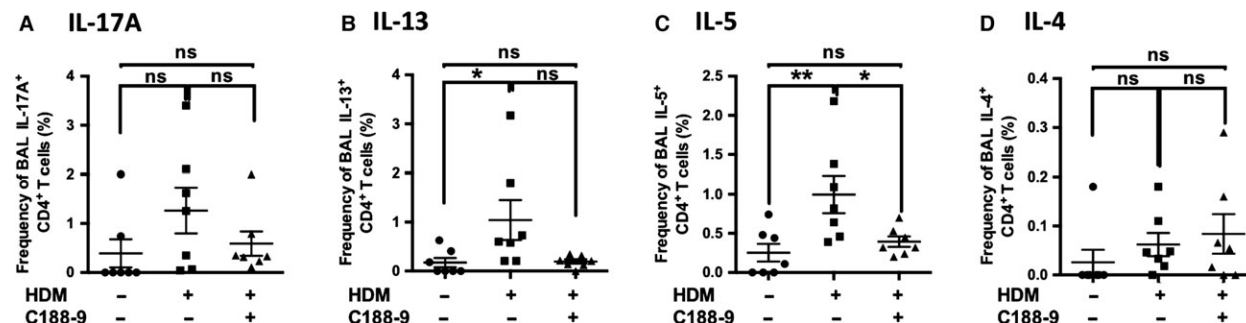


Figure 5 Effect of C188-9 treatment on the frequencies of IL-17A, IL-13, IL-5, and IL-4 expressing CD4⁺ T cells present in the bronchoalveolar lavage fluid of house dust mite-treated mice. Frequencies of Th17 and

Th2 lymphocytes were measured by flow cytometry in the bronchoalveolar lavage fluid of mice treated as indicated. Data presented are mean \pm SEM. $n \geq 6$. * $P < 0.05$, ** $P < 0.01$; ns, not significant.

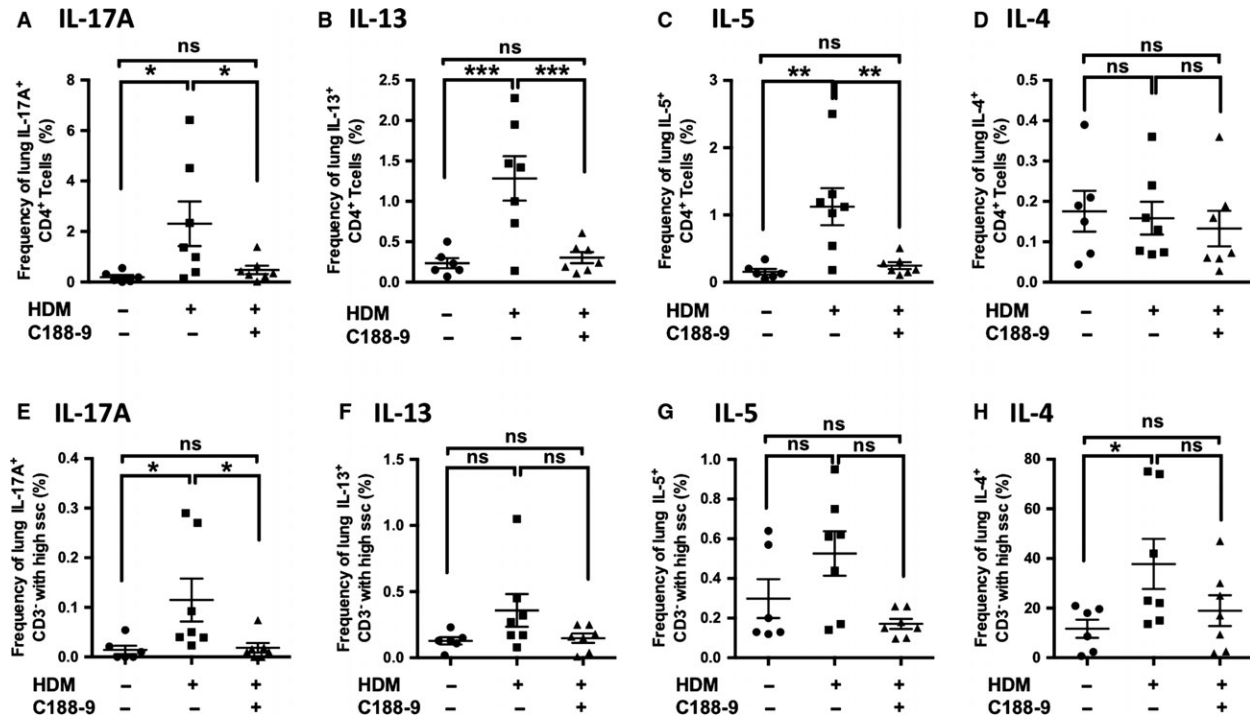


Figure 6 Effect C188-9 on the frequency of lung CD4⁺ T cells and CD3-negative cells producing IL-17A, IL-13, IL-5, and IL-4 in house dust mite-treated mice. Frequencies of CD4⁺ T cells and CD3-negative cells producing Th17 and Th2-type cytokines were measured

by flow cytometry from lungs of mice treated as indicated. Data presented are mean \pm SEM. $n \geq 6$. * $P < 0.05$, ** $P < 0.01$, *** $P < 0.001$; ns, not significant.

produced IL-17A by nearly eightfold (from 0.014 ± 0.008 to 0.11 ± 0.04 ; $P < 0.05$; Fig. 6E); the frequency of CD3-negative cells that produce IL-13 (Fig. 6F) or IL-5 (Fig. 6G) did not increase. Thus, while the major cellular sources of HDM-induced IL-13 and IL-5 were CD4⁺ T cells present in BAL fluid and in lungs, the major source of IL-4 was CD3-negative cells present in BAL fluid and lung. IL-17A was produced by both cell types: CD4⁺ T cells in lungs and CD3-negative cells present in BAL fluid. Importantly, C188-9 treatment reduced the frequency of each cytokine-producing cell that was increased by HDM within both the BAL fluid and lung to levels statistically indistinguishable from control (Fig. 5, Fig. 6, and Fig. S4).

Discussion

We demonstrated that airway inflammation and remodeling in the murine HDM model of asthma are accompanied by STAT3 activation and by increased lung levels of Th2- and Th17-type cytokines. Remarkably, systemic administration of C188-9, a small-molecule inhibitor of STAT3, completely blocked HDM-induced STAT3 activation and airway inflammation and remodeling. Inhibition of HDM-induced lung changes by C188-9 was accompanied by normalization of IL-4, IL-5, IL-13, and IL-17A cytokine levels, as well as prevention of HDM-induced increases in Th2 cells, Th17 cells, and IL-4- and IL-17A-producing non-T cells. Blocking both Th2

and Th17 pathways in mouse asthma models recently has been shown to be more effective in reducing lung inflammation compared to blocking one pathway alone, in part, by preventing compensatory over activity of the reciprocal pathway (24). Thus, a small-molecule STAT3 inhibitor such as C188-9 that targets both Th2- and Th17-cytokine production pathways represents a new therapeutic approach for asthma that may be especially beneficial.

Mice were given a 2-day holiday from inhalations of HDM and IP injections of C188-9 in each of the 3 weeks of the study to promote animal well-being and for investigator convenience. We reported previously that the plasma half-life of C188-9 is 90 min in mice following IP administration (20). Thus, the plasma levels of C188-9 would be expected to be reduced below the IC₅₀ for inhibition of cytokine-induced STAT3 phosphorylation for ~40 of the 48 h. Consequently, the finding of nearly complete normalization of pSTAT3 levels in the lungs of HDM-treated mice that received C188-9 (Fig. 1) may appear surprising at first. However, the high STAT3 binding affinity of C188-9 (4.7 ± 0.4 nM) (20) results in C188-9 accumulation within cells to levels 2.2-fold over plasma (20) and, subsequently, to reduction of pSTAT3 levels within tissues for at least 24 h (Fig. S1). An additional factor potentially contributing to pSTAT3 levels being reduced in the lungs of C188-9-treated mice given a drug holiday is that it was accompanied by a holiday from the STAT3-activating agent, HDM.

The role of STAT3 in driving Th17 cell polarization is well recognized. However, more information has emerged on the involvement of STAT3 in Th2 inflammation, as our data also support. Doganci et al. (13) and Finotto et al. (14) showed that local blockade of IL-6, the canonical interleukin that activates STAT3 and induces Th17 inflammation, decreased Th2 responses in mice. Simeone-Penney et al. (15) also showed that airway epithelium STAT3 knockout mice do not develop Th2 inflammation when exposed to HDM. Furthermore, they demonstrated that kinase blockade upstream of STAT3 diminished STAT3 activation and abrogated HDM-induced lung inflammation. The exact mechanism through which STAT3 is involved in generating Th2 cytokines is unknown and is an area of interest. Sritesky et al. (16) may have shown the most promising link. Their study illustrated that STAT3 is expressed throughout Th2 development and that mice with STAT3-deficient T lymphocytes do not develop Th2-type inflammation. They found that STAT3 binds to Th2 cell-associated gene loci (*Gata3*, *Maf*, *Batf*, and *Irf4*), thereby stabilizing STAT6-binding and allowing STAT6 to activate genes necessary for Th2 development. However, adding to the multifaceted role of STAT3 is a recent finding that its involvement in Th2 development may vary depending on where the Th2 cells are located. Lim et al. (25) demonstrated that in bronchial lymph nodes, STAT3-deficient T cells do not produce Th2 cytokines while STAT3-deficient T cells in the airways produce higher levels of Th2 cytokines. Altogether, these findings suggest that the contribution of STAT3 to Th2 development and function in allergic inflammation is expanding and becoming more complex than previously thought.

Although IL-4 was elevated in lungs and serum of HDM-treated mice, we were unable to detect significant changes in CD4⁺ T cells producing IL-4 in their lungs or BAL fluid. Further analysis of our data shows that CD3-negative cells with a high side scatter phenotype (Fig. S4B) are producing IL-4, suggesting that CD4⁺ T cells may not be the predominant or the only source of IL-4 in the house dust mite model of airway inflammation. Judging from their high side scatter phenotype, these cells may represent lung resident macrophages. Of interest, we also found that a CD3⁻ low side scatter population of cells in BAL fluid showed a 5.2-fold increase in IL-4 production ($P < 0.05$) that was reduced by ~70% by C188-9 treatment ($P < 0.05$; data not shown). As our original aim was to study CD4⁺ T cells' responses to HDM without or with C188-9, we did not include surface markers in our flow cytometry panels to identify cells other than conventional T cells. Further studies are necessary to investigate the effect of HDM without or with C188-9 on other specific cells that also produce IL-4, such as innate lymphoid cells type 2, NK cells, NKT cells, and mast cells. Regardless of their exact identity, however, our results indicated that C188-9 was able to reverse their HDM-induced production of IL-4.

In addition to IL-4, lung non-CD3⁺ cells also constituted an important source of IL-17A. Leukocytes of the innate immune system have been shown to produce IL-17A in

response to inflammation (26–28). Similar to the production of IL-4 by these cells, the production of IL-17A induced by HDM is reversed by C188-9 treatment.

Another important observation we made was that HDM administered to airways increased serum levels of IL-17A and IL-4. In parallel with CD4⁺ T-cell frequency determinations in lungs and BAL fluid, we measured lymphocyte frequencies in peripheral blood following HDM administration and detected a significant increase only in CD4⁺ IL-5⁺ T cells (data not shown). Importantly, the frequency of IL-17A- and IL-13-producing CD4⁺ T cells in peripheral blood was not altered after HDM treatment, reflecting the specificity of our flow cytometry findings in lung cells and reinforcing the idea that T cells analyzed in lung homogenates represent infiltrating or resident lung lymphocytes and not contaminating circulating lymphocytes.

The finding that HDM-induced increases in serum IL-4 and IL-17A levels were not accompanied by significant increases in peripheral blood CD4⁺ T cells producing IL-17A or IL-4 suggests that cells infiltrating the lung, or other leukocytes in the peripheral blood, were the source(s) of these cytokines rather than circulating lymphocytes. It has been previously suggested that peripheral blood levels of Th17 and Th2 cytokines may reflect the cytokine milieu in the lungs (29), which has raised the possibility of using serum studies to determine the predominant cytokines in asthmatic lungs for the purpose of categorizing a patient's phenotype and formulating cytokine-targeted therapy. At this time, however, there are still conflicting reports regarding whether serum Th17 and Th2 cytokine levels dependably reflect the pulmonary environment (30–33) with our findings indicating that this is not the case.

Lastly, it is well established that the murine model of HDM-induced asthma causes Th2 inflammation, but its effect on Th17 inflammation has remained inconsistent (34). Our findings support the conclusion that both pathways of inflammation are activated in this model, parallel to the findings of other investigators. For instance, Hubeaue et al. (35) showed that mice develop robust IL-17 responses after several weeks of HDM exposure. In the purified OVA-induced asthma model, which only elicits Th2 responses, Th17 inflammation was activated only after additional exposure to HDM, further supporting HDM's ability to induce Th17 inflammation (36). It appears that the Der p constituent of HDM induces Th2 responses, while proteases and LPS constituents preferentially activate Th17 inflammation (37). Thus, the use of lyophilized HDM extract to induce asthma is validated in our studies as an allergen to examine both inflammatory pathways of interest.

Author contributions

Aries C. Gavino performed the mouse HDM models, the microscopic analysis of the lung, the Luminex analyte measurements and analysis, and wrote the draft of the manuscript. Karen Nahmod performed the cytometric studies and analysis, and wrote sections in the manuscript describing

this work. Uddalak Bharadwaj provided Figure S1, which demonstrated the specificity of C188-9 for STAT3 vs STAT5 and STAT6. George Makedonas designed the cytometric studies, provided laboratory resources, and oversaw the flow cytometric analysis. David J. Twardy had the idea to examine the contribution of STAT3 to HDM-induced asthma, designed the experiment, provided the lab resources, provided the C188-9, oversaw the analysis of the microscopic and Luminex data, and edited the manuscript.

Conflicts of interest

David J. Twardy has filed a total of 16 patents based on work performed on C188-9 and related compounds while at Baylor College of Medicine. These patents have been licensed exclusively to StemMed, Ltd. Aries C. Gavino, Karen Nahmod, Uddalak Bharadwaj, and George Makedonas have no conflicts of interest.

Supporting Information

Additional Supporting Information may be found in the online version of this article:

Figure S1. Administration of C188-9 IP results in sustained reduction in pY-STAT3 levels in tissue. Levels of pSTAT3 and GAPDH were determined in lysates of tumor xenografts (XG) obtained from mice that received vehicle control or C188-9 (50 mg/kg) IP, as indicated ($n = 6$), 24 h prior to sacrifice. The pSTAT3/GAPDH ratio in each tumor was normalized to the mean of vehicle controls and plotted for each group; P -value for the difference between groups is indicated.

References

- Akinbami LJ, Moorman JE, Bailey C, Zahran HS, King M, Johnson CA et al. *Trends in Asthma Prevalence, Health Care Use, and Mortality In the United States, 2001–e2010*. NCHS data brief, no 94. Hyattsville, MD: National Center for Health Statistics, 2012.
- Fahy JV. Eosinophilic and neutrophilic inflammation in asthma: insights from clinical studies. *Proc Am Thorac Soc* 2009;**6**:256–259.
- Wenzel SE. Asthma: defining of the persistent adult phenotypes. *Lancet* 2006;**368**:804–813.
- Lin T, Poon AH, Hamid Q. Asthma phenotypes and endotypes. *Curr Opin Pulm Med* 2013;**19**:18–23.
- Proceedings of the ATS workshop on refractory asthma: current understanding, recommendations, and unanswered questions. *Am J Respir Crit Care Med* 2000;**162**:2341–2351.
- Al-Ramili W, Prefontaine D, Chouiali F, Martin JG, Olivenstein R, Lemiere C et al. T(H)17-associated cytokines (IL-17A and IL-17F) in severe asthma. *J Allergy Clin Immunol* 2009;**123**:1185–1187.
- McKinley L, Alcorn JF, Peterson A, Dupont RB, Kapadia S, Logar A et al. Th17 cells mediate steroid-resistant airway inflammation and airway hyperresponsiveness in mice. *J Immunol* 2008;**181**:4089–4097.
- Newcomb DC, Peebles RS Jr. Th-17 mediated inflammation in asthma. *Curr Opin Immunol* 2013;**25**:755–760.
- Harris TJ, Grosso JF, Yen H, Xie H, Kortylewski M, Albesiano E et al. Cutting edge: an in vivo requirement for STAT3 signaling in Th17 development and Th17-dependent autoimmunity. *J Immunol* 2007;**179**:4333–4337.
- Zhou L, Ivanov II, Spolski R, Min R, Sanderov K, Egawa T et al. IL-6 programs T(H)-17 cell differentiation by promoting sequential engagement of the IL-21 and IL-23 pathways. *Nat Immunol* 2007;**8**:967–974.
- Sakaguchi M, Oka M, Iwasaki T, Fukami Y, Nishigori C. Role and regulation of STAT3 phosphorylation at Ser727 in melanocytes and melanoma cells. *J Invest Dermatol* 2012;**132**:1877–1885.
- Darnell JE Jr. STATs and gene regulation. *Science* 1997;**227**:1630–1635.
- Doganci A, Eigenbrod T, Krug N, De Sanctis GT, Hausding M, Erpenbeck VJ et al. The IL-6R alpha chain controls lung CD4⁺CD25⁺ Treg development and function during allergic airway inflammation in vivo. *J Clin Invest* 2005;**115**:313–325.
- Finotto S, Eigenbrod T, Karwot R, Boross I, Doganci A, Ito H et al. Local blockade of IL-6R signaling induces lung CD4⁺ T cell apoptosis in a murine model of asthma via regulatory T cells. *Int Immunol* 2007;**19**:685–693.
- Simeone-Penney MC, Svergnini M, Tu P, Homer RJ, Mariana TJ, Cohn L et al. Airway epithelial STAT3 is required for allergic inflammation in a murine model of asthma. *J Immunol* 2007;**178**:6191–6199.
- Stritesky GL, Muthukrishnan R, Sehra S, Goswami R, Pham D, Travers J et al. The transcription factor STAT3 is required for T

Figure S2. Specificity of C188-9 for STAT3 vs STAT5 and STAT6 in human respiratory epithelial cells. In panel A, levels of pSTAT3 (top panel), pSTAT5 (middle panel), and pSTAT6 (bottom panel) were measured in lysates from asynchronous cultures of the indicated HNSCC cell lines and primary human esophageal epithelial cells (HEEPiC; used as a negative control), along with levels of GAPDH. Levels of each pSTAT were normalized to GAPDH; results shown are the mean \pm SEM of 2–4 lysates per cell line. A dashed line indicates the mean of the control cell line; the arrows indicate two HNSCC cell lines (SQ-20B & SCC-35) whose mean pSTAT3/5/6 levels were higher than control. In panel B, SQ-20B cells (top panel) and SCC-35 cells (bottom panel) were incubated with C188-9 (30 μ M) or vehicle control (DMSO) for the indicated times; lysates were prepared and assayed in duplicate for pSTAT3/5/6 and GAPDH levels. The results were normalized to GAPDH and plotted as a percentage of the time zero level; data shown are mean \pm SD.

Figure S3. C188-9 and HDM administration protocol.

Figure S4. Effect of C188-9 on the frequency of IL17-A and IL-4 expressing CD3-negative cells with high side scatter. Frequencies of CD3-negative cells with high side scatter producing IL-17A or IL-4 were measured by flow cytometry from BAL fluid of mice treated as indicated. Data presented are mean \pm SEM. $n \geq 6$. * $P < 0.05$, ** $P < 0.01$; ns, not significant.

Figure S5. Flow cytometry gating strategy. Cell suspensions from bronchoalveolar lavage (BAL) fluid and lung were stained as indicated in the Methods and gated as indicated for singularity (far-left panel), viability (center-left panel), and CD3-positivity (center-right panel). CD3⁺ cells were further gated for CD4⁺ and CD8-positivity (far-right panel).

- helper 2 cell development. *Immunity* 2011;**34**:39–49.
17. Redell MS, Ruiz MJ, Alonzo TA, Gerbing RB, Tweardy DJ. Stat3 signaling in acute myeloid leukemia: ligand-dependent and -independent activation and induction of apoptosis by a novel small-molecule Stat3 inhibitor. *Blood* 2011;**117**:5701–5709.
 18. Zhang L, Pan J, Dong Y, Tweardy DJ, Dong Y, Garibotto G et al. Stat3 activation links a C/EBP δ to myostatin pathway to stimulate loss of muscle mass. *Cell Metab* 2013;**18**:368–379.
 19. Silva KAS, Dong J, Dong Y, Dong Y, Schor N, Tweardy DJ et al. Inhibition of Stat3 activation suppresses caspase-3 and the ubiquitin-proteasome system, leading to preservation of muscle mass in cancer cachexia. *J Biol Chem* 2015;**290**:11177–11187.
 20. Bharadwaj U, Eckols TK, Xu X, Kasembeli MM, Chen Y, Adachi M et al. Small-molecule inhibition of STAT3 in radioresistant head and neck squamous cell carcinoma. *Oncotarget*, 2016;**7**:26307–26330.
 21. Hersperger AR, Makedonas G, Betts MR. Flow cytometric detection of perforin upregulation in human CD8 T cells. *Cytometry* 2008;**73A**:1050–1057.
 22. Park SY, Jing X, Gupta D, Dziarski R. Peptidoglycan recognition protein 1 enhances experimental asthma by promoting Th2 and Th17 and limiting regulatory T cell and plasmacytoid dendritic cell responses. *J Immunol* 2013;**190**:3480–3492.
 23. Yao X, Dai C, Fredriksson K, Dagur PK, McCoy JP, Qu X et al. 5A, an apolipoprotein A-1 mimetic peptide, attenuates the induction of house dust mite-induced asthma. *J Immunol* 2011;**186**:576–583.
 24. Choy DF, Hart KM, Borthwick LA, Shikotra A, Nagarkar DR, Siddiqui S et al. Th2 and Th17 inflammatory pathways are reciprocally regulated in asthma. *Sci Transl Med* 2015;**7**:301ra129.
 25. Lim H, Cho M, Choi G, Na H, Chung Y. Dynamic control of Th2 cell responses by Stat3 during allergic lung inflammation in mice. *Int Immunopharmacol* 2015;**S1567–5769**:00153–00158.
 26. Li L, Huang L, Vergis AL, Ye H, Bajwa A, Narayan V et al. IL-17 produced by neutrophils regulates IFN- γ -mediated neutrophil migration in mouse kidney ischemia-reperfusion injury. *J Clin Invest* 2010;**120**:331–342.
 27. Ferretti S, Bonneau O, Dubois GR, Jones CE, Trifilieff A. IL-17, produced by lymphocytes and neutrophils, is necessary for lipopolysaccharide-induced airway neutrophilia: IL-15 as a possible trigger. *J Immunol* 2003;**170**:2016–12.
 28. Cua DJ, Tato CM. Innate IL-17 producing cells: the sentinels of the immune system. *Nat Rev Immunol* 2010;**10**:479–489.
 29. Simarro M, Giannattasio G, Xing W, Lundquist EM, Stewart S, Stevens RL et al. The translational repressor T-cell intracellular antigen-1 (TIA-1) is a key modulator of Th2 and Th17 responses driving pulmonary inflammation induced by exposure to house dust mite. *Immunology Lett* 2012;**146**:8–14.
 30. Lee YC, Lee KH, Lee HB, Rhee YK. Serum levels of interleukins (IL)-4, IL-5, IL-13 and interferon-gamma in acute asthma. *J Asthma* 2001;**38**:665–671.
 31. Bajoruniene I, Malakauskas K, Lavinskiene S, Jeroch J, Gasiuniene E, Vitkauskienė A et al. Response of peripheral blood Th17 cells to inhaled Dermatophagoides pteronyssinus in patients with allergic rhinitis and asthma. *Lung* 2012;**190**:487–495.
 32. Davoodi P, Mahesh PA, Holla AD, Vijayakumar GS, Jayaraj BS, Chandrashekara S et al. Serum levels of interleukin-13 and interferon-gamma from adult patients with asthma in Mysore. *Cytokine* 2012;**60**:431–437.
 33. Joseph J, Benedict S, Safa W, Joseph M. Serum interleukin-5 levels are elevated in mild and moderate persistent asthma irrespective of regular inhaled glucocorticoid therapy. *BCM Pulm Med* 2004;**4**:2.
 34. Phipps S, Lam CE, Kaiko GE, Sy Foo, Col-lison A, Mattes J et al. Toll/IL-1 signaling is critical for house dust mite-specific helper T cell type 2 and type 17 responses. *Am J Respir Crit Care Med* 2009;**179**:883–893.
 35. Hubeau C, Kubera J, Hammerman K, Wright J, Denz M, Juang Y-T et al. Modulation of IL-17A and TL1A largely abrogates house dust mite-induced lung inflammation in a murine model of allergic airway disease. *J Inflamm* 2013;**10**(Suppl 1): P3.
 36. Lan F, Liu K, Zhang J, Qi Y, Li K, Lin P. Th17 response is augmented in OVA-induced asthmatic mice exposed to HDM. *Med Sci Monit* 2011;**17**:BR132–BR138.
 37. Kim YK, Oh SY, Jeon SG, Park HW, Lee SY, Chun EY et al. Airway exposure levels of lipopolysaccharide determine type 1 versus type 2 experimental asthma. *J Immunol* 2007;**178**:5375–5382.